JACS
JOURNAL OF THE AMERICAN CHEMICAL SOCIETY
Article
pubs.acs.org/JACS

Non-exponential Length Dependence of Conductance in Iodide-Terminated Oligothiophene Single-Molecule Tunneling Junctions

Limin Xiang,[†,§,#] Thomas Hines,[†,#] Julio L. Palma,[†,§] Xuefeng Lu,[‡] Vladimiro Mujica,[§] Mark A. Ratner,[∥] Gang Zhou,[*,‡] and Nongjian Tao[*,†,⊥]

[†]Center for Biosensors and Bioelectronics, Biodesign Institute, Arizona State University, Tempe, Arizona 85287, United States
[‡]Laboratory of Advanced Materials, Fudan University, Shanghai 200438, P.R. China
[§]School of Molecular Sciences, Arizona State University, Tempe, Arizona 85287, United States
[∥]Department of Chemistry, Northwestern University, Evanston, Illinois 60208, United States
[⊥]School of Electrical, Computer and Energy Engineering, Arizona State University, Tempe, Arizona 85287, United States

Supporting Information

ABSTRACT: An exponential decrease of molecular conductance with length has been observed in most molecular systems reported to date, and has been taken as a signature of non-resonant tunneling as the conduction mechanism. Surprisingly, the conductance of iodide-terminated oligothiophene molecules presented herein does not follow the simple exponential length dependence. The lack of temperature dependence in the conductance indicates that tunneling still dominates the conduction mechanism in the molecules. Transition voltage spectroscopy shows that the tunneling barrier of the oligothiophene decreases with length, but the decrease is insufficient to explain the non-exponential length dependence. X-ray photoelectron spectroscopy, stretching length measurement, and theoretical calculations show that the non-exponential length dependence is due to a transition in the binding geometry of the molecule to the electrodes in the molecular junctions as the length increases.

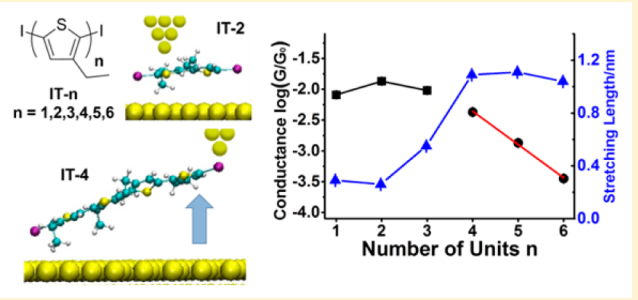

INTRODUCTION

Understanding the charge transport mechanism in molecules is a basic task in molecular and organic electronics.[1−6] For relatively small molecules, non-resonant tunneling is believed to be responsible for charge transport,[7−13] and the conductance depends on molecular length according to

$$G = G_c\, e^{-\beta L} \quad (1)$$

where G_c is the contact conductance arising from the molecule−electrode contact, L is the molecular length, and β is the decay constant that depends on the tunneling barrier of the molecular junction.[14] For most molecular systems reported to date, the tunneling barrier, and thus β, does not change appreciably with molecular length, and the conductance decays exponentially with length.[13] For this reason, exponential dependence of conductance on length has been taken as a signature of tunneling. As molecular length increases, a different charge transport mechanism known as thermally activated hopping begins to dominate, and consequently the conductance decreases inversely with molecular length, slower than exponential decay.[4,15−18] Studying the dependence of molecular conductance on length provides critical insights into the charge transport mechanism in molecules.

Conjugated oligomers, such as oligothiophenes, are important organic semiconductor materials due to their efficient charge transport along the highly conjugated π-orbitals of the oligomers.[19] Several groups have studied charge transport in oligothiophenes with different side groups and terminal groups.[20−25] Some reported exponential decay in oligothiophene conductance with molecular length,[20,23] while others found significant deviations from the exponential decay.[21,22,25] For example, Xu et al.[26] studied electrochemical gate-controlled charge transport in oligothiophene terminated with thiol linkers, and found that oligothiophene with 4 repeating units was more conductive than that with 3 repeating units. They attributed the observation to the difference in the HOMO alignment relative to the Fermi level of gold electrodes. Another recent study showed that water molecules could gate the charge transport through oligothiophene molecules with 1, 2, 3, and 5 repeating thiophene units, leading to "conductance saturation", in which the molecules have similar conductance values regardless of the lengths.[21] More recently, it was suggested that conformational changes in the oligothiophene molecules occurred during the STM break junction experiments, causing a conductance increase from 3-mer to 4-mer oligothiophene.[25]

Received: November 10, 2015
Published: December 22, 2015

DOI: 10.1021/jacs.5b11605
J. Am. Chem. Soc. 2016, 138, 679−687

Here we report a systematic study of charge transport in iodide-terminated oligothiophene with different lengths (denoted **IT-*n*** with n = 1–6, Figure 1a). We find that the conductance of the molecule changes little from **IT-1** to **IT-3**, and decays exponentially only for longer molecules, from **IT-4** to **IT-6**. To elucidate this peculiar molecular length dependence, we measure temperature dependence of conductance, current–voltage (I–V) characteristics, and transition voltage spectroscopy (TVS) of these molecules. The lack of temperature dependence in the conductance and the exponential decay for longer molecules support that non-resonant tunneling still dominates charge transport in the molecular system. Both TVS measured on single-molecular junctions, and UV–vis optical absorption spectroscopy of the molecules in bulk solution, reveal a decrease in the tunneling barrier height with molecular length, but the decrease is too small to account for the peculiar length dependence of conductance from **IT-1** to **IT-3**. We further carry out X-ray photoelectron spectroscopy (XPS) analysis on the iodide-terminated oligothiophene molecules, and find a transition in the binding geometry of the molecules on Au electrode at n = 3. This result is supported by that the stretching length of the molecular junctions exhibits an abrupt increase at n = 3. Based on the experimental evidence, we attribute the non-exponential length dependence of conductance to the transition in the binding geometry. The shorter iodide-terminated oligothiophene molecules lie flat on the electrode, and charge transport occurs via the contact of the gold electrodes with the π-orbitals of the molecules. In contrast, the longer molecules connect to the substrate and tip electrodes via gold–iodine interactions at the two terminals of the molecules, and charge transport occurs along the molecules from one terminal to another. Finally, we perform theoretical calculations, which confirm the transition in binding geometry of the molecules, and also the exponential decay of conductance with length for longer oligothiophene molecules.

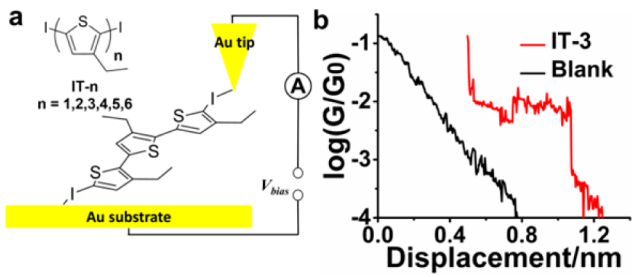

Figure 1. Conductance measurements of iodo-terminated oligothiophene with STM break-junction. (a) Structures of oligothiophene molecules terminated with iodo groups (denoted as **IT-*n***) studied here. **IT-3** bridged between a Au STM tip and a Au substrate via Au–I bonds is sketched to illustrate one of the possible molecule–electrode binding geometries. (b) Representative current–distance trace on a semi-logarithmic plot (current converted to conductance, and G_0 = 77.48 μS is the quantum conductance) for **IT-3** in mesitylene (red curve), showing a plateau regime. The black curve is a current–distance trace in blank mesitylene without **IT-3**.

RESULTS AND DISCUSSION

The oligomers studied here consist of 3-ethyl-substituted thiophene rings, varying form from 1 to 6 repeating units. Each is terminated with two iodo groups. Synthetic routes and ^{1}H NMR data can be found in the Supporting Information, part 1. We measured the conductance of the molecules using the STM break junction method with gold substrate and tip as electrodes.[27,28] Before each experiment, a control experiment was performed with a blank gold substrate in mesitylene, and the transient current–distance traces exhibited smooth decay curves (e.g., black curve in Figure 1b). Once the gold substrate was verified to be clean, a 1 mM solution of the oligothiophene molecules dissolved in mesitylene was added to the STM solution cell. The molecules attached to the substrate (Figure 1a), and subsequent current–distance traces often show plateaus, signaling the formation of single-molecule junctions (red curve in Figure 1b). Approximately 5000 current–distance traces were recorded in each measurement, from which a conductance histogram was constructed (Figure 2a). The peak

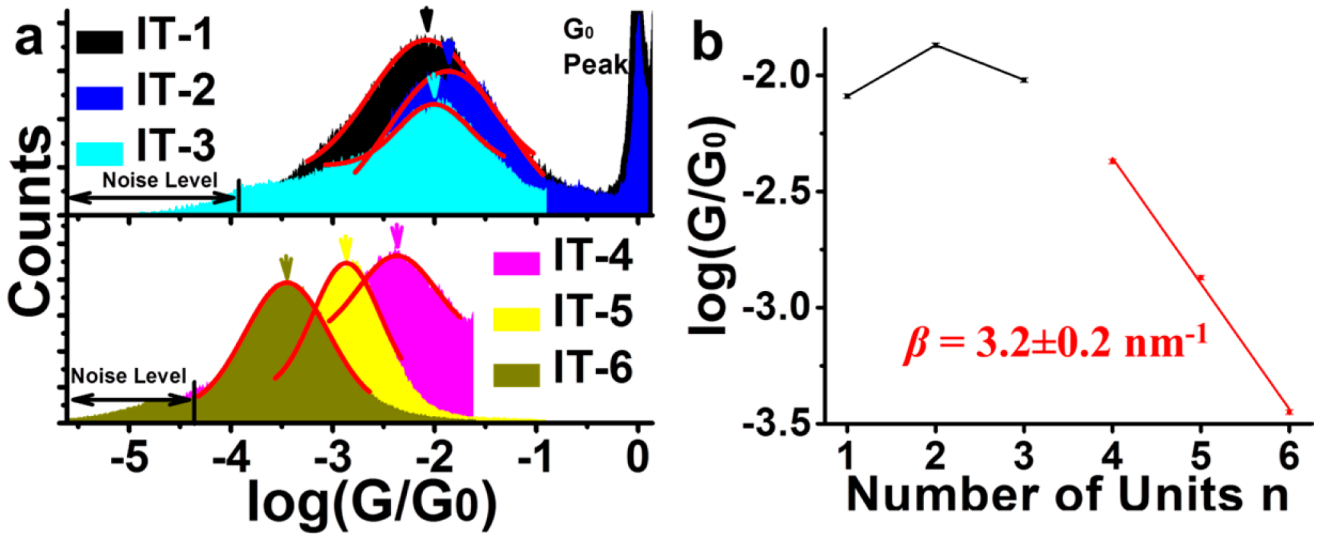

Figure 2. Conductance histograms and length dependence. (a) Conductance histograms of **IT-*n*** with n = 1, 2, 3, 4, 5, and 6, where the red curves are Gaussian fittings to the histograms. (b) Conductance in semi-logarithmic scale vs molecular length (n), showing slight changes in conductance when n = 1, 2, and 3 (black square), but exponentially decay with a decay constant, β = 3.2 ± 0.2 nm^{-1}, when n > 4 (red circle). Error bars represent the errors in the Gaussian fitting of the conductance histograms.

DOI: 10.1021/jacs.5b11605
J. Am. Chem. Soc. 2016, 138, 679–687

Table 1. Summary of All Data for Oligothiophene Molecules Presented in This Work

	peak position, $\log(G/G_0)$	fwhm	calcd $\log(G/G_0)$	stretching length (nm)	transition voltage (V)	HOMO−LUMO gap (eV)	I $3d_{5/2}$ in XPS (eV)
IT-1	−2.09 ± 0.01	1.31		0.29 ± 0.02	0.81 ± 0.01	4.64	619.3
IT-2	−1.87 ± 0.01	1.38		0.26 ± 0.01	0.66 ± 0.02	3.83	619.2
IT-3[a]	−2.02 ± 0.01	0.83		0.55 ± 0.02	0.65 ± 0.03	3.50	619.3
IT-4	−2.37 ± 0.01	0.90	−2.37	1.09 ± 0.02	0.61 ± 0.02	3.26	619.4
							621.3
IT-5	−2.87 ± 0.01	0.77	−2.86	1.11 ± 0.01	0.48 ± 0.02	3.11	
IT-6	−3.45 ± 0.01	0.97	−3.33	1.04 ± 0.01	0.50 ± 0.02	3.01	

[a]Conductance histogram of **IT-3** can be fitted with two Gaussian peaks. A possible shoulder was observed in XPS. See Supporting Information, part 9, for further discussion on the binding geometry of **IT-3**.

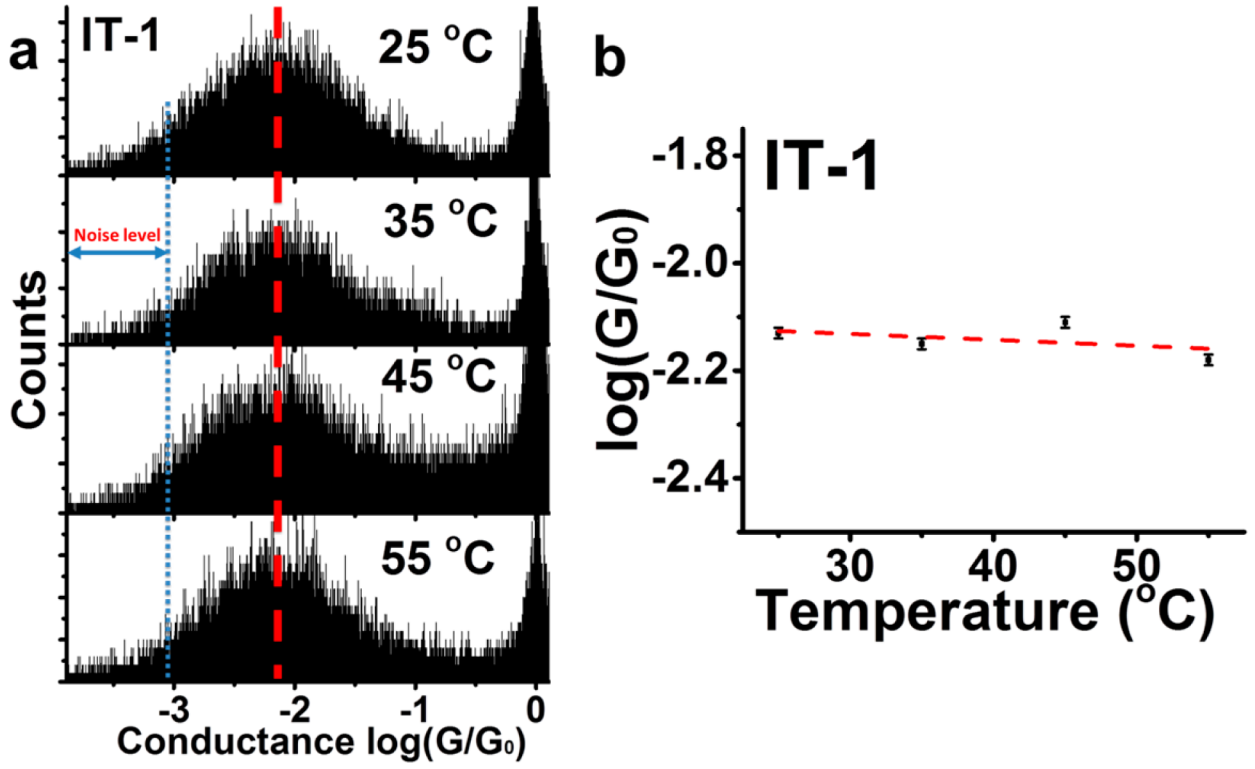

Figure 3. Temperature dependence measurement. (a) Conductance histograms of **IT-1** at 25, 35, 45, and 55 °C, showing little temperature dependence. (b) Conductance vs temperature, where the error bars are errors in the Gaussian fittings of the conductance histograms. The weak temperature dependence indicates that tunneling is the charge transport mechanism in the molecules.

in the histogram was fitted with a Gaussian distribution, where the peak position (arrows in Figure 2a) indicates the most probable conductance value of the molecule (The shoulders at lower conductance range in the histograms are due to the noise current from the circuits. See "noise level" in Figure 2a. This was also observed in blank mesitylene experiment in Figure S4a in Supporting Information, part 4). The width describes the broad distribution in the conductance of the molecule, which is originated from the variation in the molecule−electrode contact coupling, and dependence of the conductance on the couplings.[29−31] We note that the broad histogram is an inherent property of single-molecule measurement, rather than experimental error. The error bar in the most probable conductance was determined from the fitting error of the peak to Gaussian.[32] The peak positions and widths from fitting of the histograms are listed in Table 1.

Figure 2b plots the conductance of the oligothiophene as a function of molecular length. The most striking feature is that the molecular length dependence does not follow a simple exponential decay as expected for non-resonant tunneling. For short oligomers (n = 1, 2, and 3), the conductance changes only slightly with length, which is in contrast to the exponential decay observed in most molecular systems studied to date.[13] For longer oligomers (n = 4, 5, and 6), the conductance does decay exponentially with molecular length with a decay constant, β = 3.2 ± 0.2 nm^{-1}. This decay constant is consistent with reported β for similar systems.[13,21,25] Since the exponential decay of conductance with length has been used as a signature of coherent tunneling-dominated charge transport,[33] the significant deviation from the exponential decay for the short oligothiophene molecules calls for further study.

Thermally activated hopping could lead to weaker length dependence in the molecular conductance than exponential decay. To determine if tunneling or hopping dominates charge transport in the oligothiophene molecules, we carried out temperature-dependent conductance measurements for **IT-1**, **IT-3**, and **IT-5**. Figure 3a shows the conductance histograms of **IT-1** at different temperatures (see Supporting Information, part 2, for other molecules). The conductance vs temperature is plotted in Figure 3b, which shows that the conductance does

DOI: 10.1021/jacs.5b11605
J. Am. Chem. Soc. 2016, 138, 679−687

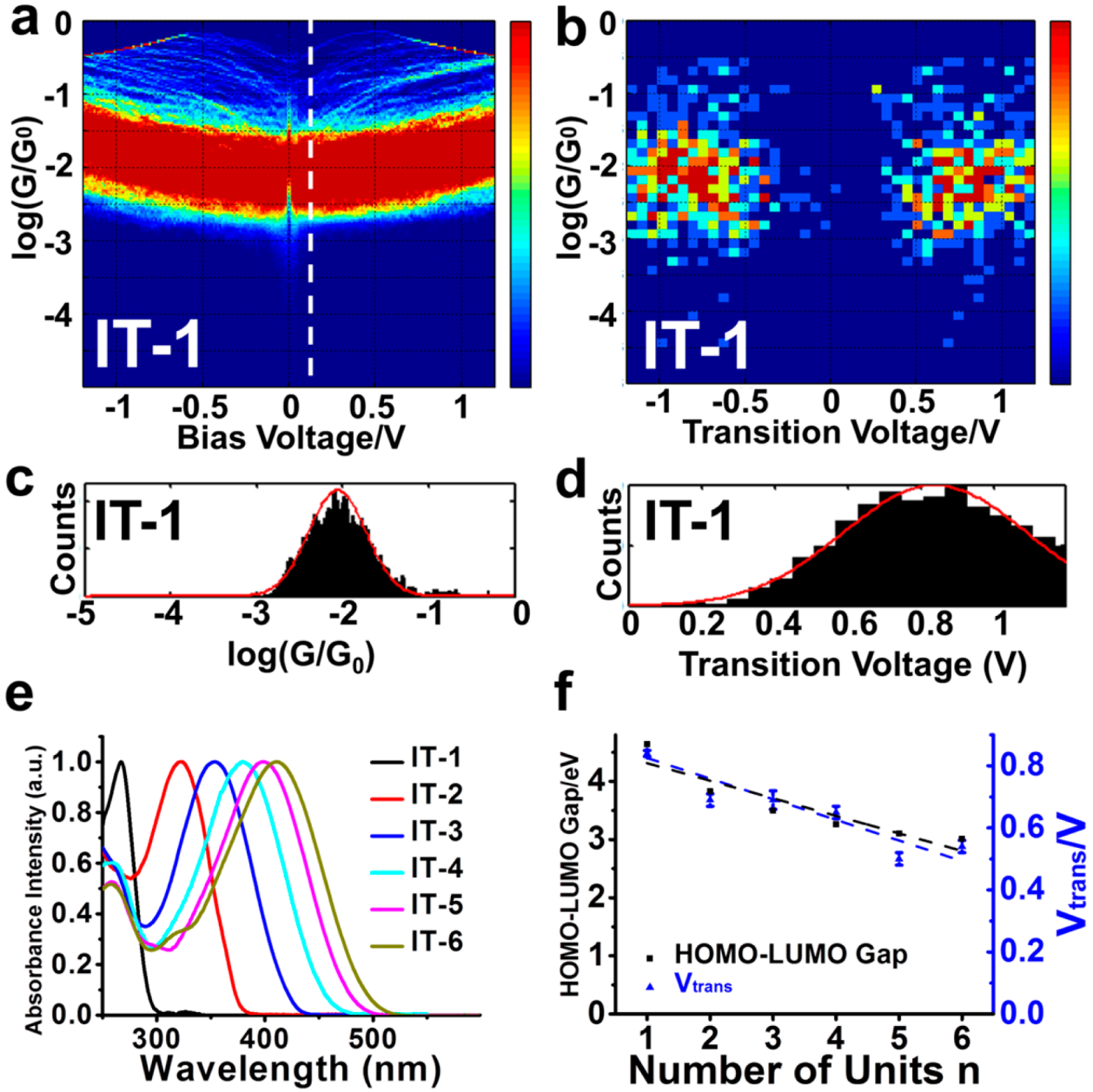

Figure 4. Transition voltage spectroscopy and UV−vis absorption spectroscopy. (a) 2D conductance−voltage (G−V) histogram. (b) 2D transition voltage histogram. (c) 1D conductance histogram at a bias of +0.1 V (vertical dashed line in panel a). The peak was fitted by a Gaussian distribution (red curve), and the peak position was taken as the conductance. (d) 1D transition voltage histogram at positive bias obtained from the 2D transition voltage histogram in panel b. The peak was fitted by a Gaussian distribution (red curve), and the peak position was taken as transition voltage. (e) Normalized UV−vis absorption spectra for **IT-*n*** in dichloromethane. (f) HOMO−LUMO gap vs n, where the black squares are from the absorption peaks in panel e, and the blue triangles are from the transition voltage histograms. Error bars are the fitting errors in the Gaussian fitting of the 1D transition voltage histograms.

not depend on temperature. The lack of strong temperature dependence indicates that thermally activated hopping does not dominate charge transport in the oligomers,[4] and tunneling is still responsible for charge transport in these molecules. This conclusion is expected for short molecules because tunneling through them is much faster than the time scales of molecular vibrations.[2] Furthermore, considering that longer oligomers (**IT-4**, **IT-5**, and **IT-6**) do follow the simple exponential decay, it is reasonable to conclude that tunneling is a dominating charge transport mechanism in the oligomers studied here.

For tunneling-dominated charge transport, the conductance is described by eq 1, which predicts a simple exponential decay only when the energy barrier is independent of molecular length. Thus, a decreasing energy barrier could explain the non-exponential length dependence of conductance.[26] Indeed, for a conjugate system like oligothiophene, the HOMO−LUMO gap is expected to decrease with molecular length. The energy level alignment depends on the interaction between the molecule and the electrode, and it is reasonable to expect that the tunneling barrier correlates with the HOMO−LUMO gap. Therefore, the energy barrier is expected to decrease as well, which could account for the observed peculiar length dependence. To examine this possibility, we studied the tunneling barrier variation with molecular length by performing

DOI: 10.1021/jacs.5b11605
J. Am. Chem. Soc. 2016, 138, 679−687

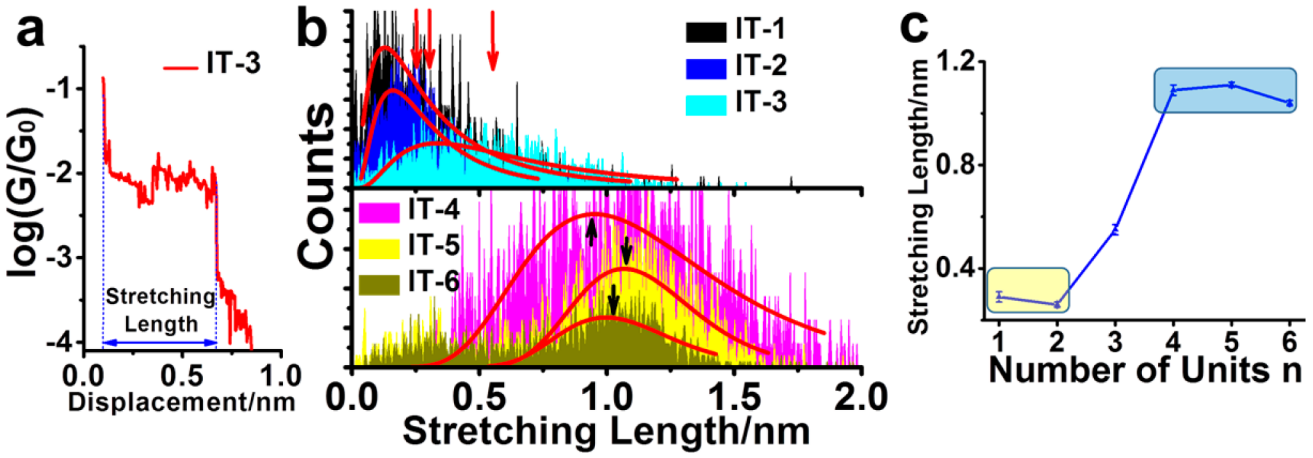

Figure 5. Stretching length analysis. (a) Stretching length is the distance over which a molecular junction can be stretched before break, which corresponds to the length of the conductance plateau in the current−distance traces. (b) Stretching length histograms of **IT-*n*** and fitting to a log-normal distribution (red lines), where the arrows indicate the mean values of the stretching length. (c) Stretching length vs *n*, showing short stretching lengths for **IT-1** and **IT-2** (yellow shaded area) and long stretching lengths for **IT-4**, **IT-5**, and **IT-6** (blue shaded area). Error bars are the fitting errors in the log-normal fitting of the stretching length histograms.

TVS[34−36] on single-molecular junctions. The method, as described elsewhere by Guo et al.,[37] measures thousands of $I-V$ curves of single molecules, from which a 2D conductance vs voltage ($G-V$) histogram is obtained (Figure 4a). The conductance histogram at each bias voltage was extracted to examine bias dependence of the conductance (Figure 4c). The conductance at low bias (+0.1 V) agrees with that obtained from the current−distance traces shown in Figure 2b, but it increases with bias due to nonlinear $I-V$ characteristics. From each $I-V$ curve, we created a plot of $\ln(G/V)$ vs $1/V$, which displays a minimum point, and the corresponding voltage at the minimum is called transition voltage (V_{trans}) of the tunneling junction. The V_{trans} is important because it is an indicator of the barrier height for a non-resonant tunneling transport mechanism.[34−36,38−42] By extracting the V_{trans} values from the individual $G-V$ curves, we constructed a 2D transition voltage histogram for **IT-1** (Figure 4b), showing distributions of both conductance and V_{trans} for the single-molecule junctions repeatedly created in the STM break junction experiment. To determine V_{trans} for each molecule, we first obtained 1D transition voltage histograms (e.g., Figure 4d) from the 2D conductance vs transition voltage histograms (e.g., Figure 4b), and then fitted each with a Gaussian function to extract V_{trans} from the peak position. Details on the data collection, $G-V$, and TVS histograms for other molecules are presented in the Supporting Information, part 3.

Figure 4f plots the transition voltage vs molecular length, which reveals a gradual decrease in the transition voltage from 0.81 to 0.65 V from **IT-1** to **IT-3**, indicating a decrease in the tunneling barrier with molecular length. To confirm this result, we also performed UV−vis absorption spectroscopy on the molecules dissolved in bulk solution, revealing red shift in the optical absorption wavelength (Figure 4e), which is consistent with the report by Capozzi et al.[25] The observed good correlation between the transition voltage and UV−vis spectroscopy data further confirmed the expectation of the correlation between the HOMO−LUMO gap and the tunneling barrier height. The observed overall decrease in the tunneling barrier with molecular length is only ∼30%, which does not significantly change β, and thus conductance is still expected to follow the exponential decay with length according to eq 1. In other words, the peculiar length dependence of the oligothiophene conductance is not due to length dependent tunneling barrier.

Exponential decay of conductance with molecular length assumes charge transports along the entire length of the molecule, which occurs only if the substrate and tip electrodes bind to the two terminal groups of the molecule. To examine if the molecule−electrode binding geometry plays a role in the observed peculiar length dependence of conductance, we studied stretching length for the oligothiophene molecules with different molecular lengths. The stretching length is the length of the plateau in the current−distance trace (see Figure 5a), which measures how long a molecular junction can be stretched before breakdown of the molecular junction, and thus provides insights into the molecule−electrode binding geometry. Figure 5b plots the stretching length histograms of the oligothiophene with different molecular lengths. The peak position of each stretching length histogram indicates the most probable stretching length (see Table 1 and Figure 5c), which was determined by fitting the histogram with a log-normal distribution. The stretching lengths for the oligomers fall into two groups, short for **IT-1** to **IT-2** (∼0.29 nm) and long for **IT-4**, **IT-5**, and **IT-6** (∼1 nm), with a transition at **IT-3**. Moreover, the widths of the conductance histograms (Figure 2a) also fall into the two groups, wide for **IT-1** to **IT-2** (full width at half-maximum (fwhm) ≈ 1.3) and narrow for **IT-3**, **IT-4**, **IT-5**, and **IT-6** (fwhm ≈ 0.9, see Table 1), with a transition at **IT-3**. It has been shown that the peak width in the conductance histogram strongly depends on the molecule-metal coupling strength.[29] The stretching length data and conductance histogram width suggest that the peculiar molecular length dependence of the oligothiophene conductance is originated from a change in the molecule−electrode binding geometry.

To gain direct information on molecule−electrode binding geometry, we carried out X-ray photoelectron spectroscopy (XPS) study of the oligothiophene with different molecular lengths on Au electrode. Because the iodo group has not been studied as a linker group for molecular junctions before, this study also helps identify the binding nature of the iodo-terminated molecules with Au electrodes. Figure 6 shows the I $3d_{5/2}$ region of XPS for **IT-2** and **IT-4**, respectively. Control

DOI: 10.1021/jacs.5b11605
J. Am. Chem. Soc. 2016, 138, 679−687

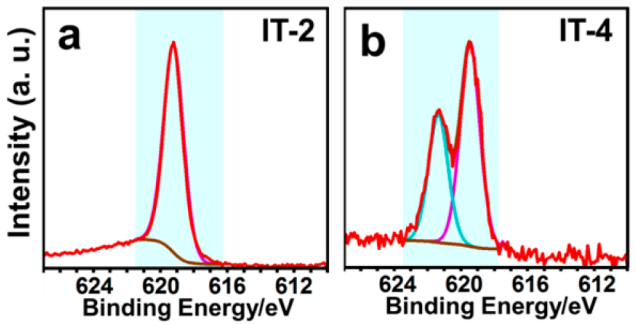

Figure 6. XPS analysis in I $3d_{5/2}$ regime of Au surfaces modified by **IT-2** (a) and **IT-4** (b). The doublet peak in panel b indicates two distinct iodine species with binding energies for iodine in C−I bond (centered at 621.3 eV)[45−47] and in Au−I−C bond (centered at 619.4 eV),[43−46] respectively. The brown line is the nonlinear Shirley background subtraction.

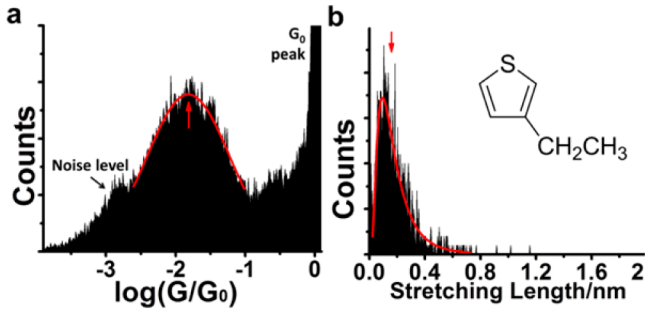

Figure 7. Conductance and stretching length for 3-ethyl thiophene. (a) Conductance histogram for 3-ethyl thiophene. The peak was fitted by a Gaussian distribution (red curve), and the peak position (red arrow) was taken as the conductance. (b) Stretching length histogram for 3-ethyl thiophene fitted with a log-normal distribution (red lines); the mean value (red arrow) was taken as the stretching length. Both the conductance and stretching length histograms of 3-ethyl thiophene are similar to those of **IT-1**, indicating that the terminal iodo groups are not involved in the molecular junctions of **IT-1**.

experiment with mesitylene is presented in Figure S5b, which shows no peaks above noise level. For **IT-2** (also see Figure S5a for **IT-1**) there is a well-defined peak at 619.2 eV, which is characteristic of iodine−gold binding.[43−46] This observation shows that the two iodo groups in **IT-1** and **IT-2** both bind to Au electrodes, suggesting that **IT-1** and **IT-2** lie flat on Au electrode. In contrast, the I $3d_{5/2}$ region has two peaks for **IT-4**, one is located at 619.4 eV, similar to that for **IT-1** and **IT-2**, and another at 621.3 eV, corresponding to weak or no binding of the iodo group with Au.[45−47] These data lead us to conclude that for **IT-4** one iodo group binds to Au electrode, but the second iodo group is not attached to the electrode. Note also that the binding energy of the 619.4 eV peak is higher than that of the Au−I^-/I_2 bond (618.4 eV),[47,48] indicating the formation of a Au−I−C contact without cleaving the C−I bond. The integrity of the C−I bond was also confirmed by electrochemical cyclic voltammograms, UV−vis absorption spectroscopy, and ^{1}H NMR of the molecules before and after its interaction with Au (see Supporting Information, part 6).

Based on the XPS data described above, we propose that the short oligothiophene molecules (e.g., **IT-1** and **IT-2**) lie flat on the Au substrate and form molecular junctions via π-orbital interactions with the Au substrate and tip electrodes (see Figure 8a). This π-orbital interaction with Au has been reported by several groups.[49−52] Because the charge transport in this binding geometry takes place via the π-electron in a thiophene ring, we expect similar conductance for **IT-1** and **IT-2**, which explains the weak length dependence of the conductance for short oligomers (n = 1, 2, and 3). This interpretation also explains naturally the relatively short stretching lengths for **IT-1** and **IT-2**. To further verify this interpretation, we carried out the conductance measurement on 3-ethyl thiophene, a molecule that is similar to **IT-1** except for the lack of two iodo groups. We found that the conductance and stretching length for 3-ethyl thiophene are similar to those of **IT-1** and **IT-2** (Figure 7), which provides direct support to the formation of molecular junctions via π-orbital interactions with the Au substrate and tip electrodes, rather than via the iodo groups for **IT-1** and **IT-2**.

The XPS data showed that as the molecular length increases (e.g., **IT-4**, **IT-5**, and **IT-6**), one iodo group begins to detach from the Au surface, making it highly probable to form a molecular junction with one end attached to the substrate electrode and the other end attached to the tip electrode in the STM break junction measurement (Figure 8b). In this case, charge transport takes place along the entire length of the molecule in the junction, which explains the exponential decay of the conductance with molecular length. This binding geometry in the molecular junctions also explains the much longer stretching length (~1 nm) for **IT-4**, **IT-5**, and **IT-6**. This long stretching length has also been observed for other molecules,[25,53−55] and consists of two contributions. One is from the stretching of Au−Au bonds,[56] which has also been reported for other strong binding terminated groups.[25,54,55] The second contribution is due to the change in the tilt angle of the molecule and the Au surface, which allows the junction to bridge between the electrodes for a longer period of time during tip withdrawal and has been observed in π-conjugated molecules.[53]

To obtain further insight into this transition in the binding geometry, we performed geometry optimizations for **IT-*n*** on a Au (1,1,1) substrate followed by transport calculations based on first-principle and non-equilibrium Green's function formalism. Figure 8a,b shows the optimized geometries for **IT-2** and **IT-4** on the Au surface. For **IT-2**, the molecule lies flat on the substrate electrode in the molecular junction. As the molecular length increases, the tendency that one end of the molecule lifts from the substrate surface increases. The thiophene rings were not able to maintain a planar conformation, thus weakening the interactions between π-orbitals and Au. The molecules start to lift up and bind to the surface via the iodine linker only on one end. Furthermore, we performed conductance calculations for **IT-*n*** (n = 4, 5, and 6), which are shown in Figure 8c with the Au−I−C chain as the linker. The calculated conductance (purple triangles) follows an exponential decay with a β value of 2.9 ± 0.1 nm^{-1}, which is in good agreement with the experimental results.

Finally, we discuss other possible effects that may explain the length dependence in the present molecular system. Leary et al. reported that water molecules can change the conductance of molecules by 2 orders of magnitude.[21] To examine possible water effects, we performed conductance measurements of **IT-2** in dry mesitylene under dry nitrogen atmosphere, and observed no obvious differences in the conductance and stretching length histogram (Figure S7). Intermolecular π−π stacking interaction[23,31,57] may also affect the conductance and molecular length dependence. However, the strength of this π−π stacking

DOI: 10.1021/jacs.5b11605
J. Am. Chem. Soc. 2016, 138, 679−687

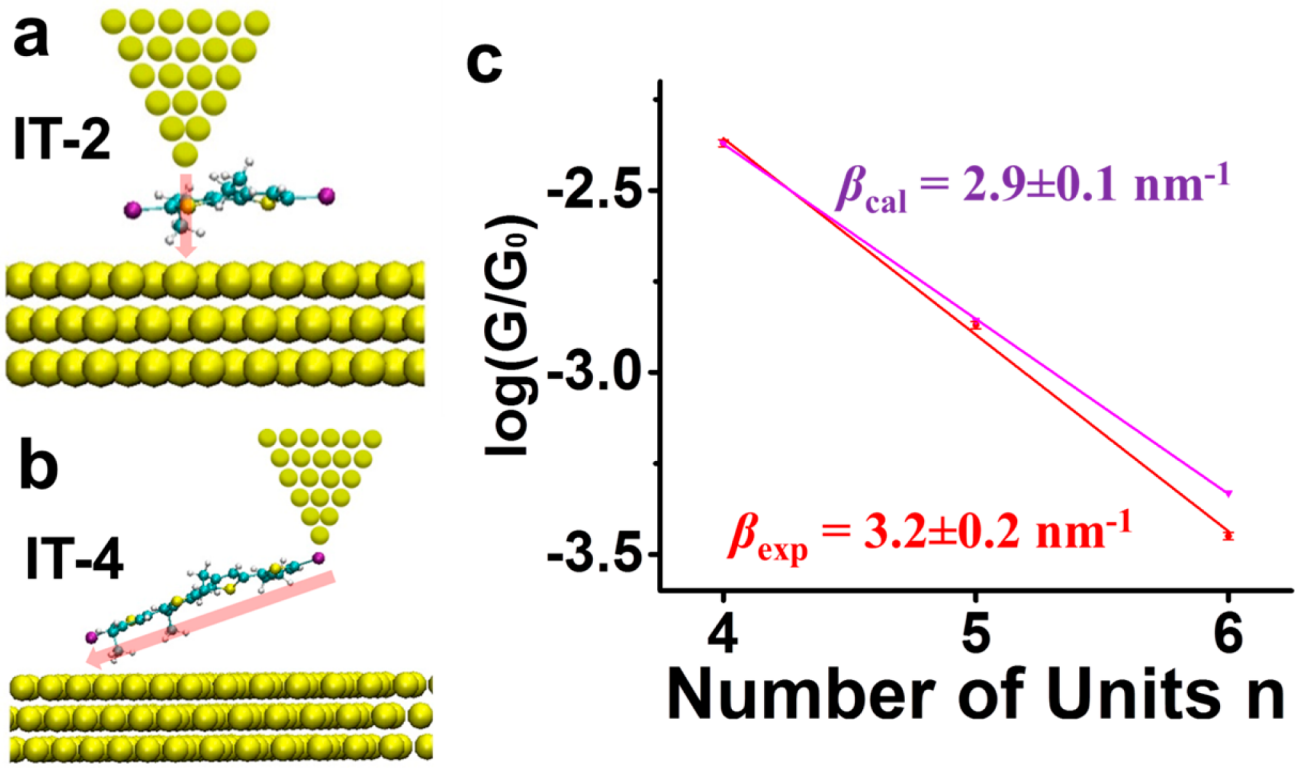

Figure 8. Calculations of the optimized geometries on a Au (111) and conductance length dependence for n = 4, 5, and 6. (a,b) Optimized geometries of **IT-2** and **IT-4** on a Au surface, showing a transition in the binding geometry. **IT-2** lies flat on the electrode but **IT-4** has a tendency to lift from the surface at one end, leading to different charge transport pathways as illustrated by the arrows. (c) Experimental (red) and calculated (purple) conductance values vs molecular length for **IT-*n*** (n = 4, 5, and 6). Note that the calculated values are normalized by the conductance of **IT-4**. Error bars are the fitting error in the Gaussian fitting of the conductance histograms.

interaction strongly depends on the conjugation extent and the molecular length.[57] Hence conductance of longer molecules will be affected, which is inconsistent with our observations. Furthermore, the strength of $\pi-\pi$ stacking interaction also depends on temperature,[58] while our study showed the conductance is independent of temperature. We also studied the effects of conformational changes to the conductance. These changes can be induced either thermally via a mechanism known as thermochromism,[59,60] or mechanically during the break junction experiments.[61] Our results show a weak temperature dependence of conductance, and calculations of rotation energy barrier (Figure S8) confirmed that thermochromism does not have a dominant effect. To examine if mechanical stretching during the STM break junction measurements affects the length dependence of conductance, we compared the conductance of unstretched junctions measured during IV sweeps when the STM tip was stationary (Figure S3g) to stretched molecular junctions measured via the standard STM break junction process (Figure 2b). The conductance vs length plots compiled from both these sets of measurements show similar length dependence and β value in both cases. This indicates that mechanically stretching does not affect the molecular conductance significantly.

CONCLUSIONS

In conclusion, we have observed peculiar length dependence in the conductance and stretching length of oligothiophene molecules (**IT-*n***) with iodo terminal groups. The conductance changes only slightly with molecular length for n = 1, 2, and 3, and the exponential decay is resumed only for longer molecules (n = 4, 5, and 6). Exponential decay of molecular conductance with length has served as a signature of coherent transport in molecular systems, and the present study shows that the exponential relation still holds, despite the observation of unusual length dependence in oligothiophene. The conductance of the molecules is independent of temperature, further indicating that tunneling remains to be the charge transport mechanism. The transition voltage measurement and UV−vis absorption spectroscopies reveal a small but systematic decrease in the effective tunneling barrier with molecular length, but the decrease is insufficient to account for the peculiar length dependence of the conductance. XPS analysis of iodine and stretching length measurements show a transition in the molecule−electrode binding geometry as the molecular length increases. For n = 1 and 2, the molecules lie flat on the substrate electrode and form molecular junctions via the π-orbitals to Au contact. For n = 4, 5, and 6, the molecules form molecular junctions via Au−I−C contact, and charge transport takes place along the entire length of the molecules from one end to another. Theoretical calculations of the optimized geometries for the molecules further confirmed that this transition is caused by a competition between the Au−I bonding and Au−π-orbitals interaction. For longer molecules ($n \geq 4$), the conductance decays with molecular length with a decay constant (β) of 3.2 ± 0.2 nm^{-1}, which is also supported by the theoretical calculation. The work shows that the conductance of a molecule is highly sensitive to the molecule−electrode contact. The actual contact may not be via the terminal linkers as intended, and electrode−molecule coupling via the π-electron could be important.

DOI: 10.1021/jacs.5b11605
J. Am. Chem. Soc. 2016, 138, 679−687

METHODS

Materials and Supplies. For synthesis, all the chemicals and reagents were purchased from commercial sources and used as received. *N*-Bromosuccinimide (NBS), *N*-iodosuccinimide (NIS), 3-ethylthiophene, *n*-butyllithium (1.6 M in hexane), trimethyl borate, and tetrakis(triphenylphosphine) palladium(0) were purchased from J&K Chemical Ltd. Mesitylene (98%) used in the STM break junction experiments was purchased from Sigma-Aldrich and dried by silica gel overnight. Gold wire (99.95%, 0.01 in. in diameter) was purchased from Alfa Aesar. Au substrate was produced by thermally evaporating ~1600 Å of gold (99.999% from Alfa Aesar) onto freshly cleaved mica slides (1 cm × 1 cm) and annealed in ultrahigh vacuum. Before each experiment, the substrate was annealed for ~1 min using a hydrogen flame.

Synthesis of Molecules. All reactions and manipulations were carried out with the use of standard inert atmosphere and Schlenk techniques. The Schlenk flasks and tubes were capped by rubber septa, and the reactions were conducted under nitrogen or argon. Anhydrous tetrahydrofuran (THF) and toluene were distilled from sodium benzophenone ketyl. Anhydrous dichloromethane (DCM) and chloroform were distilled from CaH_2. Other anhydrous solvents were distilled according to standard procedures. Stainless steel syringes were used to transfer these moisture-sensitive liquids. Proton nuclear magnetic resonance (^{1}H NMR, 400 MHz) spectra and carbon nuclear magnetic resonance (^{13}C NMR, 100 MHz) spectra were measured on a Varian Mercury Plus-400 spectrometer. Chemical shifts are reported in parts per million downfield from tetramethylsilane (TMS) and $CDCl_3$ solvent. The splitting patterns are designated as follows: s, singlet; d, doublet; t, triplet; and m, multiplet. The MALDI-TOF Mass spectra were measured on an AB SCIEX 5800 spectrometer. The UV−vis absorption spectra were measured on a dual beam scanning spectrophotometer (Shimadzu UV-2550PC) using samples prepared as dilute solutions in 1 cm quartz cuvettes.

Conductance Measurements via STM Break-Junction Technique. Experiments were performed on a Digital Instruments Nanoscope IIIA controller and a Molecular Imaging STM head/scanner. In this method, a custom written LabVIEW program modulated the tip into and out of the surface at the rate of 39 nm/s using a two set-point feedback system. In this setup, the two set-points were separated by 4 orders of magnitude. A small bias voltage (10−100 mV, positive or negative) was applied between the STM tip and Au substrate. The surface was verified to be clean by the smooth and exponential current−distance traces in mesitylene. A 1 mM solution of molecules dissolved in mesitylene was then added to the STM solution cell. A total of 5000 current−distance traces were recorded for each experiment, and conductance histograms were constructed with an algorithm.[37] The algorithm counted only the traces showing counts exceeding a preset threshold in the histograms. Stretching length histogram was constructed by compiling the all distance values for the traces recorded when the current was within a defined range including the plateau regime. Temperature of the STM cell was controlled by mounting the Au substrate onto a semiconductor cooler with a thermistor to measure the temperature (controlled by Lake Shore 331 temperature controller). The *I*−*V* measurements are described in Supporting Information, part 3.

X-ray Photoelectron Spectroscopy Analysis. Samples were prepared by immersing the Au substrate into the solution of molecules (1 mM in mesitylene) for 3 h, rinsed with mesitylene, followed by drying with high-purity nitrogen. XPS was performed on a VG ESCALAB 220i-XL with Al Kα anode (1486.6 eV) operated at 60 W and 12 kV. The X-ray takeoff angle was 45°, and the data were acquired from the region within 500 μm of the outer surface of the sample under a pressure of 10^{-8} Torr. A pass energy of 20 eV was used for high-resolution spectra with an energy resolution of 0.7 eV. C(1s) peak with a binding energy of 284.6 eV was used as the references binding energy. Peak fitting was carried out using CasaXPS2316PR1 software with a Gaussian−Lorentzian product function and a nonlinear Shirley background subtraction.

Theoretical Calculations. We performed geometry optimizations of the molecules including gold slabs consisting on three layers of Au(1,1,1). The size of the gold slabs varied according to the size of the molecule ensuring that all systems were allowed to stack on top of the slab. We used the PBE functional[62] and DZP basis set using the SIESTA code, varying the position until the force on each atom was smaller than 0.01 eV/Å. The gold atoms were fixed to reduce the computational cost.

Electron transport calculations for **IT-4** to **IT-6** systems were performed the non-equilibrium Green's function technique combined with density functional theory (NEGF-DFT)[63,64] as implemented in TranSIESTA code[63] at the DZP/PBE level of theory and zero bias. The systems were built in the traditional electrode−molecule−electrode setup. The molecular structures were taken from the geometry relaxations, and each electrode consisted of two layers of Au(1,1,1). Each layer had three sub-layers with a total of 13 gold atoms each. A cutoff energy of 300 Ry for the grid mesh was used, and 30-point contour integration on the imaginary place was calculated to obtain the density matrix.

ASSOCIATED CONTENT

Supporting Information

The Supporting Information is available free of charge on the ACS Publications website at DOI: 10.1021/jacs.5b11605.

Details of molecular synthesis, ^{1}H NMR, UV−vis data, XPS, electrochemistry CV, histograms, and theoretical calculations, including Figures S1−S9 (PDF)

AUTHOR INFORMATION

Corresponding Authors

*zhougang@fudan.edu.cn

*nongjian.tao@asu.edu

Author Contributions

#L.X. and T.H. contributed equally to this work.

Notes

The authors declare no competing financial interest.

ACKNOWLEDGMENTS

The authors thank the Office of Naval Research (N00014-11-1-0729, L.X. and J.L.P.), U.S. National Science Foundation (grant no. CHE-1105588, T.H. and N.T.), and National Natural Science Foundation of China (grant no. 51273045, X.L. and G.Z.). The authors thank LeRoy Eyring Center for Solid State Science at Arizona State University and Prof. Timothy Karcher for the help with XPS analysis.

REFERENCES

(1) Aviram, A.; Ratner, M. A. *Chem. Phys. Lett.* **1974**, *29*, 277.
(2) Nitzan, A. *Annu. Rev. Phys. Chem.* **2001**, *52*, 681.
(3) McCreery, R. L. *Chem. Mater.* **2004**, *16*, 4477.
(4) Luo, L.; Choi, S. H.; Frisbie, C. D. *Chem. Mater.* **2011**, *23*, 631.
(5) Mirjani, F.; Thijssen, J. M.; Whitesides, G. M.; Ratner, M. A. *ACS Nano* **2014**, *8*, 12428.
(6) Reed, M. A.; Zhou, C.; Deshpande, M. R.; Muller, C. J.; Burgin, T. P.; Jones, L.; Tour, J. M. *Ann. N. Y. Acad. Sci.* **1998**, *852*, 133.
(7) Joachim, C.; Ratner, M. A. *Proc. Natl. Acad. Sci. U. S. A.* **2005**, *102*, 8801.
(8) Amdursky, N.; Marchak, D.; Sepunaru, L.; Pecht, I.; Sheves, M.; Cahen, D. *Adv. Mater.* **2014**, *26*, 7142.
(9) Sedghi, G.; Esdaile, L. J.; Anderson, H. L.; Martin, S.; Bethell, D.; Higgins, S. J.; Nichols, R. J. *Adv. Mater.* **2012**, *24*, 653.
(10) Sedghi, G.; Garcia-Suarez, V. M.; Esdaile, L. J.; Anderson, H. L.; Lambert, C. J.; Martin, S.; Bethell, D.; Higgins, S. J.; Elliott, M.; Bennett, N.; Macdonald, J. E.; Nichols, R. J. *Nat. Nanotechnol.* **2011**, *6*, 517.

DOI: 10.1021/jacs.5b11605
J. Am. Chem. Soc. 2016, 138, 679−687

(11) Yan, H.; Bergren, A. J.; McCreery, R.; Della Rocca, M. L.; Martin, P.; Lafarge, P.; Lacroix, J. C. *Proc. Natl. Acad. Sci. U. S. A.* **2013**, *110*, 5326.
(12) McCreery, R. L.; Yan, H.; Bergren, A. J. *Phys. Chem. Chem. Phys.* **2013**, *15*, 1065.
(13) Metzger, R. M. *Chem. Rev.* **2015**, *115*, 5056.
(14) Simmons, J. *J. Appl. Phys.* **1963**, *34*, 1793.
(15) Ho Choi, S.; Kim, B.; Frisbie, C. D. *Science* **2008**, *320*, 1482.
(16) Xiang, L.; Palma, J. L.; Bruot, C.; Mujica, V.; Ratner, M. A.; Tao, N. *Nat. Chem.* **2015**, *7*, 221.
(17) Zhao, X.; Huang, C.; Gulcur, M.; Batsanov, A. S.; Baghernejad, M.; Hong, W.; Bryce, M. R.; Wandlowski, T. *Chem. Mater.* **2013**, *25*, 4340.
(18) Haiss, W.; Martin, S.; Scullion, L. E.; Bouffier, L.; Higgins, S. J.; Nichols, R. J. *Phys. Chem. Chem. Phys.* **2009**, *11*, 10831.
(19) Zhang, L.; Colella, N. S.; Cherniawski, B. P.; Mannsfeld, S. C. B.; Briseno, A. L. *ACS Appl. Mater. Interfaces* **2014**, *6*, 5327.
(20) Yamada, R.; Kumazawa, H.; Noutoshi, T.; Tanaka, S.; Tada, H. *Nano Lett.* **2008**, *8*, 1237.
(21) Leary, E.; Höbenreich, H.; Higgins, S. J.; van Zalinge, H.; Haiss, W.; Nichols, R. J.; Finch, C. M.; Grace, I.; Lambert, C. J.; McGrath, R.; Smerdon, J. *Phys. Rev. Lett.* **2009**, *102*, 086801.
(22) Lee, S. K.; Yamada, R.; Tanaka, S.; Chang, G. S.; Asai, Y.; Tada, H. *ACS Nano* **2012**, *6*, 5078.
(23) Ie, Y.; Endou, M.; Lee, S. K.; Yamada, R.; Tada, H.; Aso, Y. *Angew. Chem., Int. Ed.* **2011**, *50*, 11980.
(24) Zhitenev, N. B.; Meng, H.; Bao, Z. *Phys. Rev. Lett.* **2002**, *88*, 226801.
(25) Capozzi, B.; Dell, E. J.; Berkelbach, T. C.; Reichman, D. R.; Venkataraman, L.; Campos, L. M. *J. Am. Chem. Soc.* **2014**, *136*, 10486.
(26) Xu, B. Q. Q.; Li, X. L. L.; Xiao, X. Y. Y.; Sakaguchi, H.; Tao, N. J. J. *Nano Lett.* **2005**, *5*, 1491.
(27) Xu, B.; Tao, N. J. *Science* **2003**, *301*, 1221.
(28) Haiss, W.; van Zalinge, H.; Higgins, S. J.; Bethell, D.; Höbenreich, H.; Schiffrin, D. J.; Nichols, R. J. *J. Am. Chem. Soc.* **2003**, *125*, 15294.
(29) Williams, P. D.; Reuter, M. G. *J. Phys. Chem. C* **2013**, *117*, 5937.
(30) Quan, R.; Pitler, C. S.; Ratner, M. A.; Reuter, M. G. *ACS Nano* **2015**, *9*, 7704.
(31) Reuter, M. G.; Hersam, M. C.; Seideman, T.; Ratner, M. A. *Nano Lett.* **2012**, *12*, 2243.
(32) Richter, P. *Telecommun. Dat. Acqu. Progres. Rep.* **1995**, *42*−*122*, 107.
(33) Tao, N. J. *Nat. Nanotechnol.* **2006**, *1*, 173.
(34) Beebe, J. M.; Kim, B.; Gadzuk, J. W.; Daniel Frisbie, C.; Kushmerick, J. G. *Phys. Rev. Lett.* **2006**, *97*, 026801.
(35) Huisman, E. H.; Guédon, C. M.; van Wees, B. J.; van der Molen, S. J. *Nano Lett.* **2009**, *9*, 3909.
(36) Mirjani, F.; Thijssen, J. M.; van der Molen, S. J. *Phys. Rev. B: Condens. Matter Mater. Phys.* **2011**, *84*, 115402.
(37) Guo, S.; Hihath, J.; Díez-Pérez, I.; Tao, N. *J. Am. Chem. Soc.* **2011**, *133*, 19189.
(38) Kushmerick, J. *Nature* **2009**, *462*, 994.
(39) Vilan, A.; Cahen, D.; Kraisler, E. *ACS Nano* **2013**, *7*, 695.
(40) Beebe, J. M.; Kim, B.; Frisbie, C. D.; Kushmerick, J. G. *ACS Nano* **2008**, *2*, 827.
(41) Bâldea, I. *Chem. Phys.* **2010**, *377*, 15.
(42) Xie, Z.; Bâldea, I.; Smith, C. E.; Wu, Y.; Frisbie, C. D. *ACS Nano* **2015**, *9*, 8022.
(43) Berry, G. M.; Bravo, B. G.; Bothwell, M. E.; Cali, G. J.; Harris, J. E.; Mebrahtu, T.; Michelhaugh, S. L.; Rodriguez, J. F.; Soriaga, M. P. *Langmuir* **1989**, *5*, 707.
(44) Yu, Y.; Dubey, M.; Bernasek, S. L.; Dismukes, G. C. *Langmuir* **2007**, *23*, 8257.
(45) Liu, G.; Ryoo, K.; Kim, S. H. *Surf. Sci.* **2007**, *601*, 2967.
(46) Eder, G.; Smith, E. F.; Cebula, I.; Heckl, W. M.; Beton, P. H.; Lackinger, M. *ACS Nano* **2013**, *7*, 3014.
(47) Hirayama, M.; Caseri, W. R.; Suter, U. W. *J. Colloid Interface Sci.* **1998**, *202*, 167.
(48) Bravo, B. G.; Michelhaugh, S. L.; Soriaga, M. P.; Villegas, I.; Suggs, D. W.; Stickney, J. L. *J. Phys. Chem.* **1991**, *95*, 5245.
(49) Afsari, S.; Li, Z.; Borguet, E. *Angew. Chem., Int. Ed.* **2014**, *53*, 9771.
(50) Kiguchi, M.; Takahashi, T.; Takahashi, Y.; Yamauchi, Y.; Murase, T.; Fujita, M.; Tada, T.; Watanabe, S. *Angew. Chem., Int. Ed.* **2011**, *50*, 5708.
(51) Moreno-García, P.; La Rosa, A.; Kolivoška, V.; Bermejo, D.; Hong, W.; Yoshida, K.; Baghernejad, M.; Filippone, S.; Broekmann, P.; Wandlowski, T.; Martín, N. *J. Am. Chem. Soc.* **2015**, *137*, 2318.
(52) Schneebeli, S. T.; Kamenetska, M.; Cheng, Z.; Skouta, R.; Friesner, R. A.; Venkataraman, L.; Breslow, R. *J. Am. Chem. Soc.* **2011**, *133*, 2136.
(53) Diez-Perez, I.; Hihath, J.; Hines, T.; Wang, Z.-S.; Zhou, G.; Mullen, K.; Tao, N. *Nat. Nanotechnol.* **2011**, *6*, 226.
(54) Arroyo, C. R.; Leary, E.; Castellanos-Gómez, A.; Rubio-Bollinger, G.; González, M. T.; Agraït, N. *J. Am. Chem. Soc.* **2011**, *133*, 14313.
(55) Xu, B.; Xiao, X.; Tao, N. J. *J. Am. Chem. Soc.* **2003**, *125*, 16164.
(56) Yanson, A. I.; Bollinger, G. R.; van den Brom, H. E.; Agrait, N.; van Ruitenbeek, J. M. *Nature* **1998**, *395*, 783.
(57) Wu, S.; Gonzalez, M. T.; Huber, R.; Grunder, S.; Mayor, M.; Schonenberger, C.; Calame, M. *Nat. Nanotechnol.* **2008**, *3*, 569.
(58) Herz, A. H. *Adv. Colloid Interface Sci.* **1977**, *8*, 237.
(59) Yoshino, K.; Nakajima, S.; Gu, H. B.; Sugimoto, R. *Jpn. J. Appl. Phys.* **1987**, *26*, L2046.
(60) Selzer, Y.; Cabassi, M. A.; Mayer, T. S.; Allara, D. L. *J. Am. Chem. Soc.* **2004**, *126*, 4052.
(61) Dell, E. J.; Capozzi, B.; DuBay, K. H.; Berkelbach, T. C.; Moreno, J. R.; Reichman, D. R.; Venkataraman, L.; Campos, L. M. *J. Am. Chem. Soc.* **2013**, *135*, 11724.
(62) Perdew, J. P.; Burke, K.; Ernzerhof, M. *Phys. Rev. Lett.* **1996**, *77*, 3865.
(63) Brandbyge, M.; Mozos, J.-L.; Ordejón, P.; Taylor, J.; Stokbro, K. *Phys. Rev. B: Condens. Matter Mater. Phys.* **2002**, *65*, 165401.
(64) Xue, Y.; Datta, S.; Ratner, M. A. *Chem. Phys.* **2002**, *281*, 151.

DOI: 10.1021/jacs.5b11605
J. Am. Chem. Soc. 2016, 138, 679−687